Planta (2007) 227:189–197
DOI 10.1007/s00425-007-0606-z

ORIGINAL ARTICLE

Expression of animal CED-9 anti-apoptotic gene in tobacco modifies plasma membrane ion fluxes in response to salinity and oxidative stress

Sergey Shabala · Tracey A. Cuin · Luke Prismall · Lev G. Nemchinov

Received: 19 May 2007 / Accepted: 29 July 2007 / Published online: 22 August 2007

Abstract Apoptosis, one form of programmed cell death (PCD), plays an important role in mediating plant adaptive responses to the environment. Recent studies suggest that expression of animal anti-apoptotic genes in transgenic plants may significantly improve a plant's ability to tolerate a variety of biotic and abiotic stresses. The underlying cellular mechanisms of this process remain unexplored. In this study, we investigated specific ion flux "signatures" in *Nicotiana benthamiana* plants transiently expressing CED-9 anti-apoptotic gene and undergoing salt- and oxidative stresses. Using a range of electrophysiological techniques, we show that expression of CED-9 increased plant salt and oxidative stress tolerance by altering K^+ and H^+ flux patterns across the plasma membrane. Our data shows that PVX/CED-9 plants are capable of preventing stress-induced K^+ efflux from mesophyll cells, so maintaining intracellular K^+ homeostasis. We attribute these effects to the ability of CED-9 to control at least two types of K^+-permeable channels; outward-rectifying depolarization-activating K^+ channels (KOR) and non-selective cation channels (NSCC). A possible scenario linking CED-9 expression and ionic relations in plant cell is suggested. To the best of our knowledge, this study is the first to link "ion flux signatures" and mechanisms involved in regulation of PCD in plants.

S. Shabala (✉) · T. A. Cuin · L. Prismall
School of Agricultural Science,
University of Tasmania, Private Bag 54,
Hobart, TAS 7001, Australia
e-mail: Sergey.Shabala@utas.edu.au

L. G. Nemchinov (✉)
USDA/ARS, Plant Sciences Institute,
Molecular Plant Pathology Laboratory,
Beltsville, MD 20705, USA
e-mail: Lev.Nemchinov@ars.usda.gov

Keywords Membrane transport · Apoptosis · Programmed cell death · Salinity · Oxidative stress

Introduction

Apoptosis is one of the forms of programmed cell death (PCD) that induces characteristic morphological and biochemical alterations in cells and results in the orchestrated disassembly of the cell (Xu et al. 2004). Being essential for cell and tissue homeostasis and specialization (Chen and Dickman 2004), PCD also plays an important role in mediating plant adaptive responses to the environment, and was experimentally proved to occur in response to salinity, cold stress, waterlogging and hypoxia (Katsuhara and Kawasaki 1996; Pennell and Lamb 1997; Huh et al. 2002). While the regulatory mechanisms of PCD in animals are fairly well known and mostly depend on caspase protease activity (Lam et al. 2001), the apoptotic machinery and signal-transduction pathways of PCD in plants remain unclear. A key role for caspase-like proteases has been suggested (Hatsugai et al. 2004; Chichkova et al. 2004), and several reports of plant proteases with caspase-like properties that functionally mimic caspase activity in animals have been recently published (Watanabe and Lam 2004; Rojo et al. 2004).

Being upstream of the PCD signaling cascade, membrane-transport processes play a pivotal role in PCD in animal tissues (Gulbins et al. 2000; Panayiotidis et al. 2006). Thus far, no comprehensive electrophysiological study has been undertaken to investigate PCD-related membrane-transport processes in plants. However, ion fluxes are known to be the earliest detectable signaling event in plant defense responses (Clough et al. 2005). Thus, it appears that the physiological role of plant ion channels and

ion transport in PCD-related processes is as important as their activities in other cellular responses to the environment (Zimmermann et al. 1999; Khurana et al. 2005).

Recent studies have suggested that transgenic expression of animal anti-apoptotic genes may significantly improve a plant's ability to tolerate a variety of biotic and abiotic stresses (Dickman et al. 2001). Expression of animal anti-apoptotic genes suppressed the extensive plant cell death caused by pathogens, and enhanced resistance to abiotic stresses such as wounding, heat, salt, drought, cold, UV-B, and oxidative stress (Mitsuhara et al. 1999; Dickman et al. 2001; Lincoln et al. 2002; Qiao et al. 2002; Xu et al. 2004; Chen and Dickman 2004; Li and Dickman 2004). Although a direct practical application of this research is unlikely due to various social and regulatory constraints, knowledge of the mechanisms of action of these genes in plants and specifically, the role of ion flux signaling in the biological activity of apoptotic genes, may be crucial for our understanding of the role that apoptosis plays in plant stress responses.

This work is aimed at addressing the above issue. Unlike previous studies, we used transient expression of an anti-apoptotic gene CED-9 from *Caenorhabditis elegans* by means of a plant-virus-based vector. The benefits of virus-based transient gene expression versus transgenic plants include rapid engineering, high levels of desired protein and its systemic spread in plant tissues within a short period of time (Scholthof et al. 1996). Using a range of electrophysiological techniques, we show that expression of CED-9 anti-apoptotic gene in tobacco leaf mesophyll increased salt and oxidative stress tolerance by altering ion flux patterns across the plasma membrane. The identity of specific ion transporters was further investigated in pharmacological experiments. A relationship between the discovered pattern of ion signaling initiated by the activity of the anti-apoptotic gene and mechanisms of PCD in plants is discussed.

Materials and methods

Amplification and cloning of CED-9 gene into the plant virus-based vector

Copy DNA of the anti-apoptotic *C.elegans* CED-9 gene was obtained from R. Horvitz, Massachusetts Institute of Technology, Cambridge, MA, USA. PCR primers were designed based on the available CED-9 sequence to introduce the *Pme*1 restriction site (underlined) at both the 5′ and 3′ ends of the gene: 5′GTTTAAACAATGACACGCT GCACGGCGG 3′ (homologous primers) and 5′ GTTTAA ACTTACTTCAAGCTGAACATCAT 3′ (complementary primer). The PCR-amplified CED-9 gene was directly cloned into the TOPO XL vector (Invitrogen, Carlsbad, CA, USA). XL/CED-9 plasmid was digested with *Pme*I and the gel-purified CED-9 fragment was subcloned into the PVX-based vector pP2C2S (obtained from D. Baulcombe, Sainsbury Laboratory, Norwich, UK), which had been linearized with *Eco*RV and dephosphorylated with calf intestinal alkaline phosphatase (Promega, Madison, WI, USA). The resulting plasmid was designated PVX/CED-9 (Fig. 1a). The correctness of all recombinant constructs was verified by nucleotide sequencing.

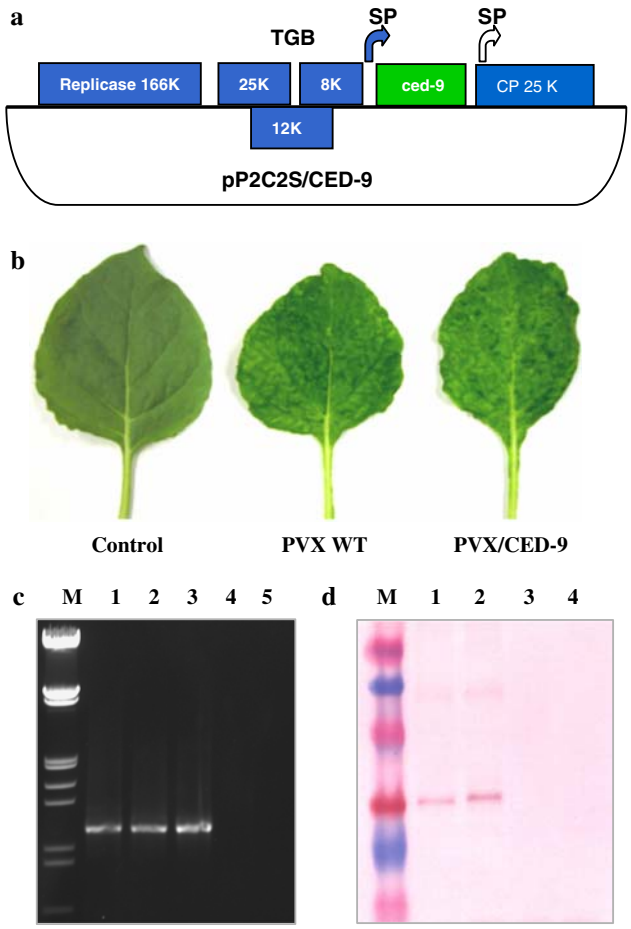

Fig. 1 **a** Diagram of PVX/CED-9 vector. *Closed arrow* duplicated PVX CP subgenomic promoter. *Open arrow* PVX CP subgenomic promoter. *TGB* triple gene block. **b** Characteristic symptoms of PVX infection on wild type and PVX/CED-9 *N. benthamiana* leaves (8 days after inoculation). **c** RT-PCR products amplified from plants infected with PVX/CED-9 using primers surrounding MCS of pP2C2S. Expected size of the PCR product is ~1.1 kb. M, Lambda DNA *Eco*RI/*Hind*III marker (Promega): 21.2, 5.1, 3.5, 2, 1.9, 1.5, 1.3, 0.9, 0.8 and 0.5 kb; 1–3, RT-PCRs from different *N. benthamiana* plants infected with PVX/CED-9; 3 and 4, RT-PCRs from plant infected with wild type (WT) PVX and from a non-inoculated plant, respectively. **d** Western blot analysis. Membranes were probed with an antibody to CED-9. M, ColorBurst Molecular weights (kDa) protein marker (Sigma): 90, 65, 40, 30, 20, 13, and 8; 1 and 2, extracts from different plants infected with PVX/CED-9; 3 and 4, extracts from plants infected with WT PVX and from non-inoculated plant, respectively

Transcript preparation and inoculation of plants

PVX/CED-9 plasmids were linearized using restriction enzyme *Spe*I, and capped transcripts were generated from cDNA clones using Ambion's T7 mMessage Machine kit (Ambion, Austin, TX, USA). The transcripts were mechanically inoculated onto fully expanded leaves of *Nicotiana benthamiana*. Inoculated plants were grown in a standard potting mix (Shabala et al. 2000) at 25°C with a 16 h light period in the containment greenhouse facilities at the School of Agricultural Science, University of Tasmania, Australia or Molecular Plant Pathology Laboratory, USDA/ARS, Beltsville, MD, USA.

Reverse transcription polymerase chain reaction (RT-PCR) and western blot analysis

Total nucleic acids were extracted from non-inoculated symptomatic leaves of *N. benthamiana* plants using TRIzol Reagent (Invitrogen, Carlsbad, CA, USA). RT and PCR were performed in a single reaction mixture using the Titan One Tube RT-PCR kit as described by the manufacturer (Roche Molecular Biochemicals, Chicago, IL, USA). The CED-9-specific primers as (above) or the following primer pair derived from the pP2C2S region surrounding multiple cloning site (MCS), were used in the amplification reaction: 5′AATCACAGTGTTGGCTTGC3′ (homologous primer) and 5′GTGGTAGTTGAGGTAGTTGAC 3′ (complementary primer). The PCR fragments were fractionated on a 0.8% agarose gel. The integrity of RT-PCR products were verified by automated nucleotide sequencing. For immmunoblot analysis, ~100 mg of leaf tissue was homogenized in 1× PBS buffer containing protease inhibitor cocktail (Sigma Chemical Co., St Louis, MO, USA), centrifuged, mixed with 2× Laemmlli loading buffer and electrophoresed on pre-cast 10–20% Tris–Glycine gels (Invitrogen), following by blotting onto a nitrocellulose membrane (Invitrogen). Membranes were probed with polyclonal antibodies to CED-9 (Santa Cruz Biotechnology Inc., Santa Cruz, CA) and developed with the BCIP/NBT Substrate System (KPL Inc., MD, USA).

Greenhouse experiments

One week after inoculation, plants were subjected to salinity stress (daily irrigation with 200 mM NaCl). The experiment was carried out as a randomized block design, with three blocks containing six treatments × 2 plants each. Visual assessment was performed on a daily basis, and stomatal conductance, leaf chlorophyll content and maximal photochemical efficiency of PSII (chlorophyll fluorescence F_v/F_m ratio) were measured from both fully matured and young (recently unfolded) tobacco leaves at the end of the experiment as described in our earlier publications (Smethurst and Shabala 2003; Pang et al. 2004).

Non-invasive ion flux measurements

Net K^+ and H^+ fluxes were measured non-invasively using the microelectrode ion flux measuring technique (MIFE; UTas Consulting Ltd, Hobart). All details on microelectrode fabrication and calibration are given elsewhere (Shabala 2000; Shabala et al. 2006). Mature, but still growing leaves showing clear visual symptoms of infection were chosen for measurements. After leaves were excised, the leaf epidermis was gently removed, and mesophyll segments of about 4 × 5 mm size were cut and left floating (peeled side down) on a surface of measuring solution (0.1 mM $CaCl_2$ + 0.2 mM KCl; pH 6 unbuffered) as described by Shabala et al. (2000) for about 3 h. One hour prior to measurement, mesophyll segments were immobilized in a Perspex holder and placed in a measuring chamber.

Electrode tips were positioned 50 μm above the leaf surface, tips aligned and separated by 3–5 μm. During measurements, electrodes were moved back and forth in a square-wave manner by a computerized stepper motor between two positions, 50 and 80 μm above the leaf surface, with 0.1 Hz frequency. Net ion fluxes were calculated from measured differences in the electrochemical potential between these two positions for each ion, as described earlier (Shabala et al. 1997; Newman 2001).

Electrophysiological protocols

Two different types of measurement were undertaken. *Transient flux kinetics* was measured in response to acute NaCl (200 mM) or H_2O_2 (1 mM) treatment applied to leaf mesophyll segments isolated from plants grown under normal conditions. Net K^+ and H^+ fluxes were measured from immobilized segments (see above) for 10 to 20 min to ensure the absence of any transient trends. A NaCl or H_2O_2 stock was then added to the measuring chamber, thoroughly mixed, and net ion flux kinetics measured for another 30–40 min. *Steady-state* net K^+ and H^+ fluxes were measured from either tobacco leaf mesophyll isolated from plants grown at 200 mM NaCl for 2 weeks, or from leaf segments treated with 0.2 mM H_2O_2 for 24 h.

Membrane potential measurements

Conventional KCl-filled Ag/AgCl microelectrodes (Cuin and Shabala 2005) with tip diameter ~0.5 μm were used. Measurements were taken from at least five individual leaf segments for each treatment. Membrane potentials were recorded for 1.5–2 min after initial cell penetration.

Pharmacology

Prior to measurement, leaf segments were pre-treated for 1 h with a range of known channel blockers or metabolic inhibitors. These included: (1) tetraethylammonium chloride (TEA^+ 20 mM); (2) gadolinium chloride (Gd^{3+} 50 μM) and (3) sodium orthovanadate (Na_2VO_4 0.5 mM). All chemicals were purchased from Sigma.

Statistical analysis

Statistical significance of mean values was determined using the standard Student's *t* test at $P < 0.05$ level.

Results

Symptoms and stability of the recombinant virus in plants

The recombinant PVX/CED-9 virus vector was infectious and caused characteristic PVX symptoms visibly indistinguishable from wild type virus (Fig. 1b). Symptoms on leaves of inoculated *N. benthamiana* plants appeared 7–10 days post-inoculation and subsequently developed into a systemic infection. The engineered virus remained stable and produced CED-9 protein for at least 1 month after inoculation (monitored by Western blotting and RT-PCR).

Transient expression of *C. elegans* CED-9 gene in plants

RT-PCR using both CED-9 specific- and pP2C2S-derived primers confirmed the presence of target CED-9 RNA in plants, as well as the recombinant nature of the PVX vector in vivo. Amplified fragments of expected size were repeatedly obtained from different *N. benthamiana* plants infected with PVX/CED-9 (Fig. 1c), and the identity of RT-PCR product was verified by nucleotide sequencing. Western blots probed with CED-9-specific antibody immunologically confirmed the presence of the CED-9 protein product in PVX/CED-9 plants: the revealed protein bands corresponded to the predicted molecular mass of CED-9 (32.1 kDa). No banding pattern was observed from plants inoculated with WT PVX or from non-inoculated plants (Fig. 1d).

CED-9 expression ameliorate detrimental salinity effects

Two weeks of salt stress (200 mM NaCl) had a significant impact on phenotype, plant growth and physiological characteristics. Both non-inoculated and WT PVX-virus plants treated with NaCl were stunted and had a large number of chlorotic leaves (Fig. 2b, c), with no apparent difference between these two treatments. At the same time, plants infected with recombinant PVX/CED-9 virus were of larger

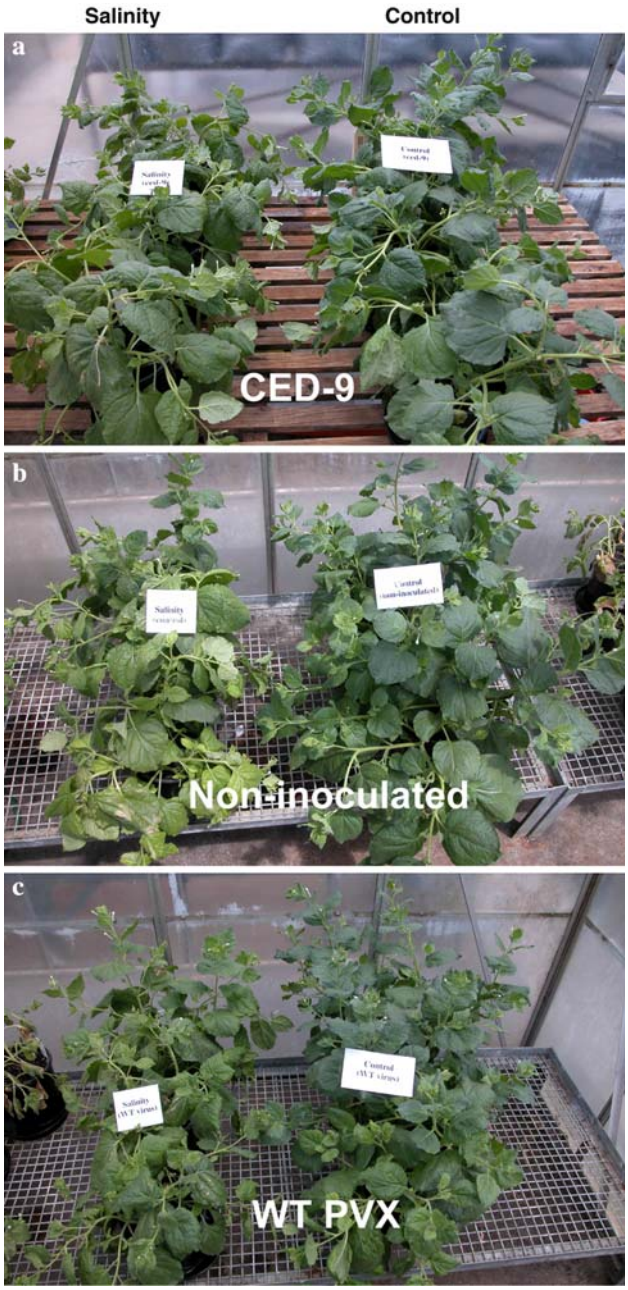

Fig. 2 Effect of salt stress (watering with 200 mM NaCl for 2 weeks) on plants expressing CED-9 gene, WT PVX and non-inoculated controls

size and looked healthier (Fig. 2a). The PVX/CED-9 plants had significantly higher amounts of chlorophyll compared with the NaCl-treated control and WT PVX plants (Fig. 3a). Interestingly, chlorophyll content was also significantly ($P < 0.05$) higher in WT PVX leaves compared with non-inoculated plants under saline conditions. The possible reason for this may be that viral infection per se caused a substantial oxidative stress in plants at the initial stages of inoculation. Thus, it is logical to expect that PVX infected plants would have better ROS scavenging

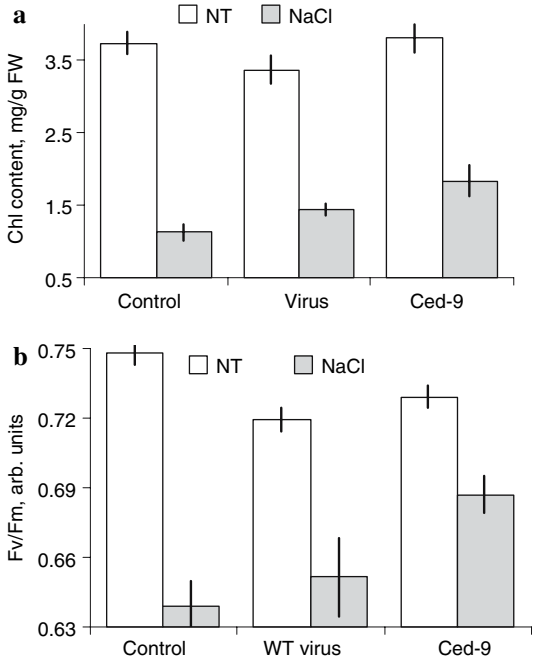

Fig. 3 Effect of salt stress on leaf photosynthetic characteristics in control leaves, leaves infected with WT PVX virus, and PVX/CED-9 leaves. **a** Total chlorophyll content; **b** maximal photochemical efficiency of PSII (F_v/F_m value). Mean ± SE (n = 6 and 12, respectively). *NT* Non-treated with NaCl; *NaCl* watered with 200 mM NaCl for 2 weeks

(detoxification) systems, and are better adapted to the subsequent salinity stress. CED-9 plants also showed significantly higher photochemical efficiency (as evident from chlorophyll fluorescence F_v/F_m values; Fig. 3b), although, no significant difference in stomatal conductance (g_s) values between control, WT PVX and CED-9 leaves was found (data not shown). NaCl caused about a 2.5-fold increase in stomatal resistance in all treatments.

CED-9 effects on NaCl-induced ion flux responses

Acute salt stress (200 mM NaCl) caused an immediate and massive K^+ efflux from tobacco mesophyll (Fig. 4a). No significant difference was found between control and WT PVX plants, while in PVX/CED-9 leaves, the magnitude of NaCl-induced K^+ efflux was significantly less (~40% reduction; Fig. 4a). Salinity treatment also induced a gradually increasing H^+ efflux (Fig. 4b). No significant difference, however, occurred in transient NaCl-induced H^+ fluxes between treatments (Fig. 4b).

When steady-state net K^+ fluxes were measured from leaf mesophyll isolated from plants irrigated for 2 weeks with 200 mM NaCl, a significant difference was apparent between control and NaCl-treated leaves in both non-inoculated plants and WT PVX leaves. At the same time, there was no significant difference between control and NaCl-treated mesophyll segments isolated from leaves of plants transiently expressing the anti-apoptotic gene (Fig. 4c). Steady-state H^+ fluxes were essentially unaffected by 2 weeks of NaCl treatment (Fig. 4d).

CED-9 effects on ROS-induced ion fluxes

Oxidative stress (1 mM H_2O_2 added to leaf mesophyll) induced a gradually increasing net K^+ efflux (Fig. 5a). In CED-9 plants, this K^+ efflux was significantly attenuated (~50% reduction compared with control and WT PVX treatments). Incubation in 0.2 mM H_2O_2 for 24 h also

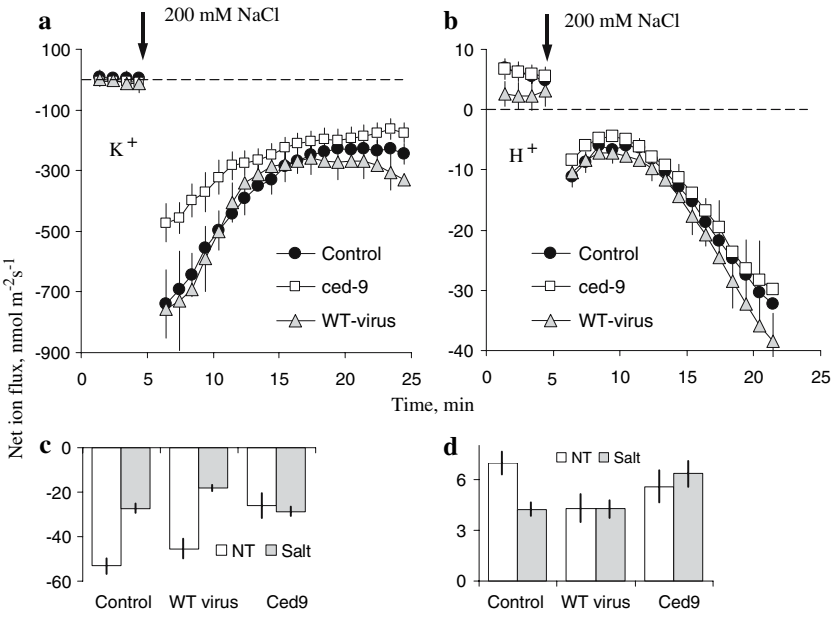

Fig. 4 Net ion fluxes measured from tobacco leaf mesophyll under saline conditions. Transient net K^+ **a** and H^+ **b** flux kinetics measured in response to acute salt stress; 200 mM NaCl was applied to leaves excised from plants grown in normal (non-saline) conditions. Mean ± SE (n = 6–8). Panels **c** and **d** show steady-state net ion K^+ **c** and H^+ **d** fluxes measured from tobacco leaf mesophyll from plants grown at 200 mM NaCl for 2 weeks. Mean ± SE (n = 30). For all ion flux measurements, the sign convention is "influx positive"

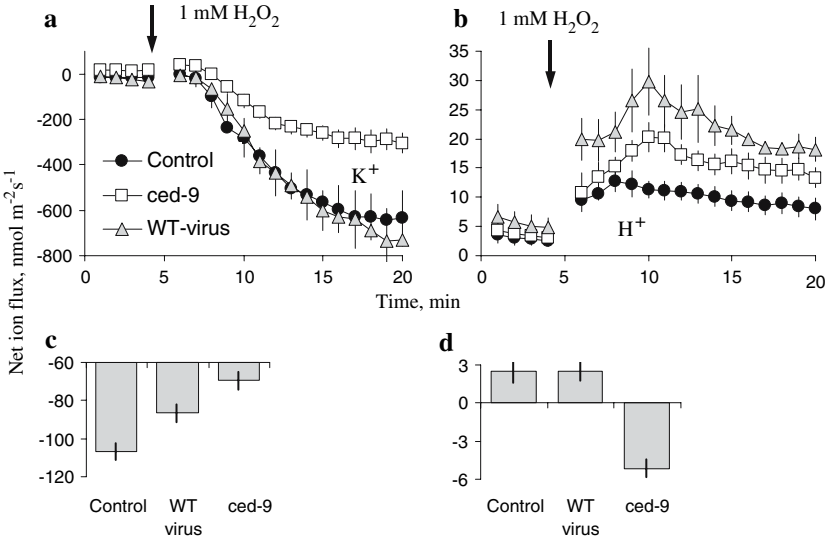

Fig. 5 Net ion fluxes measured from tobacco leaf mesophyll under oxidative stress conditions. Transient net K^+ **a** and H^+ **b** flux kinetics measured in response to acute 1 mM H_2O_2 treatment. Mean ± SE (n = 5–8). **c, d** Show steady-state net ion K^+ **c** and H^+ **d** fluxes measured from tobacco leaf mesophyll after 24 h of treatment with 0.2 mM H_2O_2. Mean ± SE (n = 30)

resulted in a pronounced K^+ leak from the cell. Consistent with the transient data, CED-9 plants had a better ability to retain K^+ in the cell (Fig. 5c). Oxidative stress also caused a pronounced transient net H^+ uptake; the magnitude of which was significantly higher in both WT PVX and CED-9 plants compared to the control (Fig. 5b). More prolonged oxidative stress (24 h in 0.2 mM H_2O_2) did not affect the magnitude of steady-state net H^+ fluxes in control (non-inoculated) and WT PVX leaves, but resulted in a pronounced H^+ efflux from CED-9 leaf mesophyll (Fig. 5d).

Pharmacology

Leaf pre-treatment in known ion channel blockers and metabolic inhibitors had a significant impact on both the steady-state net ion fluxes and on the magnitude of NaCl-induced flux transients (Fig. 6). Both TEA^+ (a known blocker of K^+-selective channels), and Gd^{3+} (a known blocker of non-selective cation channels; NSCC), significantly shifted steady-state K^+ fluxes towards net K^+ influx (Fig. 6a), with Gd^{3+} having much stronger effect. Both TEA^+ and Gd^{3+} were also efficient in suppressing NaCl-induced K^+ leak from leaf mesophyll (ca. 70 and 40 % inhibition, respectively; Fig. 6b). The effect of inhibitors was qualitatively similar in both non-inoculated and CED-9 plants (Fig. 6). Leaf pre-treatment in 0.5 mM vanadate (a known inhibitor of H^+-ATPase), also significantly suppressed the magnitude of peak H^+ flux response (data not shown), indicating a possible involvement of the plasma membrane H^+-pump in mediating NaCl-induced net H^+ fluxes.

Membrane potential changes

Consistent with previous reports (Shabala et al. 2003, 2005, 2006), NaCl-treated leaves were significantly depolarized

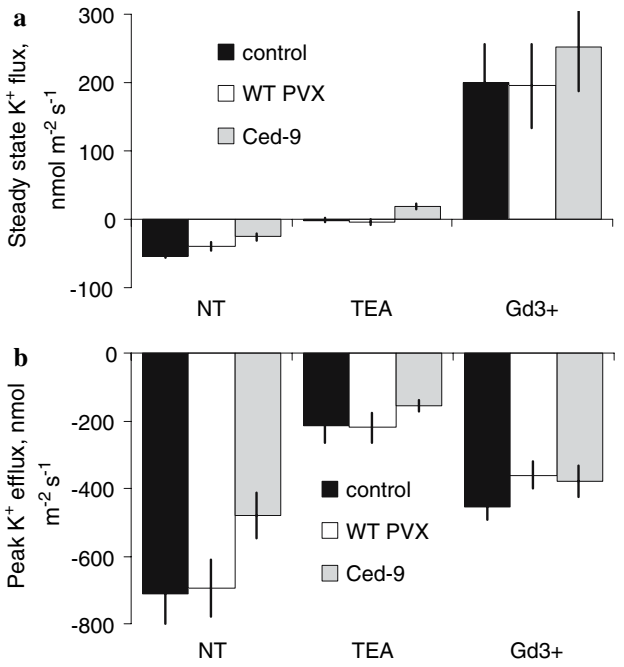

Fig. 6 Pharmacology of salt-induced (200 mM NaCl) ion flux responses from tobacco leaf mesophyll. Steady-state net K^+ fluxes **a** and peak K^+ efflux **b** are shown from control and PVX/CED-9 leaves after 1 h of pre-treatment in 20 mM TEACl or 50 μM $GdCl_3$. *NT* Not-treated leaves (no inhibitors used). Mean ± SE (n = 5–7)

compared with non-treated leaves. However, the magnitude of this depolarization was dramatically different between treatments (Table 1). While in the control and WT PVX plants, two weeks of irrigation with 200 mM NaCl resulted in a dramatic membrane depolarization (by 50.7 ± 3.2 and 65.2 ± 4 mV, respectively), in CED-9 leaves, the magnitude of this depolarization was only 9.8 ± 3.5 mV (Table 1). Qualitatively similar results were found for oxidative stress; 24 h of 0.2% H_2O_2 treatment significantly

Table 1 Steady-state values of membrane potential of tobacco mesophyll cells in control and plants irrigated with 200 mM NaCl for 2 weeks

	Control	NaCl
Non-inoculated	-132.9 ± 1.4^{a}	-82.2 ± 3.2^{d}
WT PVX	-139.2 ± 4.1^{a}	-74 ± 1.7^{d}
CED-9	-109.2 ± 3.5^{b}	-99.6 ± 0.9^{c}

Mean ± SE ($n = 30$). Numbers with different letters are significantly different at $P < 0.05$

depolarized the plasma membrane of control and WT PVX mesophyll cells (by 8.2 ± 1.4 and 18.5 ± 1.3 mV, respectively), but hyperpolarized the membrane of CED-9 cells (by 6.6 ± 1.3 mV). These findings implicate the involvement of voltage-sensitive ion transporters in mediating both NaCl- and ROS-induced stress responses.

Discussion

CED-9 anti-apoptotic genes enhance plant salt tolerance by preventing NaCl-induced K^+ efflux from salinised leaf tissues

Given the central role of membrane-transport process in PCD, surprisingly little is known about specific ion transporters mediating this process and the possible effects of anti-apoptotic genes on their activity. Earlier Qiao et al. (2002) showed that NaCl treatment disrupted cell vacuole, and that expression of an anti-apoptotic Bcl-xl gene significantly delayed this process in tobacco suspension cells by some "unknown mechanism". Both salt-sensitive mutants of yeast (*cnb1Δ*) and *Arabidopsis* (*sos1*) exhibited substantially more profound PCD symptoms, indicating that salt-induced PCD is mediated by ion disequilibrium (Huh et al. 2002). Yet, no electrophysiological evidence was presented.

One of the earliest detectible responses to salt stress is a massive K^+ efflux, observed in both root (Shabala et al. 2003, 2005, 2006; Cuin and Shabala 2005; Chen et al. 2005) and leaf (Shabala 2000; Shabala et al. 2000, 2006) tissue. Such a large K^+ efflux reduces the intracellular K^+ pool (Cuin et al. 2003; Carden et al. 2003), significantly impairing cell metabolism. Consistent with the key role of K^+ homeostasis in salt-tolerance mechanisms (Maathuis and Amtmann 1999), a reduction of K^+ efflux correlates with increased salt-tolerance (Carden et al. 2003; Chen et al. 2005, 2007). In this work, we report that *N. benthamiana* plants, transiently expressing CED-9 anti-apoptotic gene from *C. elegans*, conferred higher salt tolerance (Figs. 2, 3). We attribute this to the ability of CED-9-expressing cells to better maintain intracellular K^+ homeostasis by preventing NaCl-induced K^+ leak from salinized leaf tissue (Fig. 4a). Consistent with the transient K^+ flux data (Fig. 4a), CED-9 leaves showed the smallest steady-state K^+ efflux in control (no salt) conditions (Fig. 4b). Assuming a cytosolic K^+ concentration of around 150 mM (Cuin et al. 2003), the Nernst potential value for 0.2 mM K^+ in the bath (as in this study) is $E_K = -167$ mV. At the same time, membrane potential values in all treatments did not exceed −140 mV (Table 1), favoring passive K^+ efflux under our experimental conditions. The fact that CED-9 leaves had the smallest K^+ efflux (Fig. 4c), despite having the least negative membrane potential (Table 1), implies an ability of CED-9 cells to efficiently control plasma membrane K^+ efflux channels, as well as a direct involvement of plasma membrane K^+ efflux channels in salt stress-induced PCD in plants.

CED-9 controls both specific K^+-permeable and NSCC channels in mesophyll plasma membrane

Our previous studies have suggested that NaCl-induced K^+ efflux across the plasma membrane is mediated by at least two transport systems, namely outward-rectifying K^+ permeable channels (KOR) and non-selective cation (NSCC) channels (Shabala et al. 2005, 2006). CED-9 appears to affect the activity of both these K^+-transport systems. Pharmacological experiments suggested that steady-state net K^+ flux was mediated mainly by Gd^{3+}-sensitive NSCC channels (Fig. 6a), while NaCl-induced K^+ efflux was dominated by KOR channels (as evident from TEA^+ experiments; Fig. 6b), with a relatively smaller contribution from NSCC (Fig. 6b). These pharmacological results are in a good accordance with membrane potential data (Table 1). The observed ~40% reduction in the magnitude of NaCl-induced K^+ efflux in CED-9 plants (Fig. 4a) can be attributed to a much less membrane depolarization (9.8 ± 3.5 vs. 50.7 ± 3.2 mV for CED-9 and control, respectively; Table 1), implicating the involvement of voltage-sensitive KOR channels in the regulation of PCD and anti-apoptotic activity of CED-9.

CED-9 ameliorates detrimental effects of oxidative stress on plasma membrane transporters

Reactive oxygen species (ROS) are known to be primarily responsible for the impairment of cellular function under numerous abiotic and biotic stress conditions, including salinity (Zhu 2002). It has been suggested that anti-apoptotic genes suppress ROS generation in chloroplasts and mitochondria (Pennell and Lamb 1997; Xu et al. 2004). However, these conclusions are based on visual observations such as a lack of decoloration in transgenic leaves under stress conditions (e.g. Xu et al. 2004; Qiao et al. 2002). Here we report that a transiently expressed anti-apoptotic

CED-9 gene increased total chlorophyll content in salt stressed leaves (Fig. 3a), resulting in substantially higher leaf photosynthetic activity (Fig. 3b). We attribute these effects to the ability of the anti-apoptotic gene to control ionic homeostasis in ROS stressed cells (Fig. 5).

Increased ROS production has been long known to detrimentally affect cellular ionic homeostasis by causing lipid peroxidation and impairing membrane integrity, making membranes more permeable to electrolytes and, specifically, to K^+ (McKersie et al. 1982). At the same time, chlorophyll biosynthesis is critically dependent on the intracellular K^+ level (Marschner 1995). Here we show that, as a result of H_2O_2 treatment, tobacco mesophyll cells had a clearly pronounced K^+ efflux (Fig. 5a, c), and that CED-9 plants were capable of significantly attenuating this detrimental effect of oxidative stress in both short-term (Fig. 5a) and long-term (Fig. 5c) experiments. This can explain the higher photosynthetic activity (Fig. 3b) and chlorophyll content (Fig. 3a) in PVX/CED-9 plants compared to control or WT PVX.

Based on our data, the following tentative scenario can be offered. Under saline conditions, Na^+ enters the cell through NSCC, causing (amongst other things), a significant membrane depolarization and ROS production (especially in green photosynthesizing cells). This will result in a dramatic reduction of the cytosolic K^+ pool, caused by a massive K^+ efflux through both depolarization-activated KOR channels (Shabala et al. 2006) and ROS-activated (Demidchik et al. 2003) NSCC channels. In animal tissues, caspase activity is significantly increased by a low cytosolic K^+ content (Hughes and Cidlowski 1999). Assuming plant caspase-like proteases are regulated in a similar way, a decrease in cytosolic K^+ pool may activate caspase-like proteases, leading to Programmed Cell Death. Accordingly, a plausible explanation for the ameliorating effect of animal anti-apoptotic CED-9 genes is that their expression in the leaf mesophyll may block (either directly or indirectly) the permeability of NSCC, reducing Na^+ uptake into the cell and preventing NaCl-induced depolarization and the resulting K^+ leak through KOR. In addition, CED-9 blockage of the KOR is also possible. Altogether, this maintains the optimal intracellular K^+ homeostasis and prevents activation of caspase-like proteases (and, hence, PCD).

In summary, this work represents the first attempt to link ion flux "signatures" and apoptosis in plants. We have shown that expression of animal anti-apoptotic CED-9 gene in tobacco leaf mesophyll caused a significant alteration in cell electrophysiological characteristics and, specifically, activity of plasma membrane K^+ and H^+ transporters. The specific nature of these transporters should be further investigated in patch-clamp experiments and by expressing anti-apoptotic genes in *Arabidopsis* knock-out mutants.

Acknowledgments This work has been supported by the ARC Discovery and Tasmanian Institute of Agricultural Research grants (S.S.) and by the United States Department of Agriculture, Agricultural Research Service (L.N.).

References

Carden DE, Walker DJ, Flowers TJ, Miller AJ (2003) Single-cell measurements of the contributions of cytosolic Na^+ and K^+ to salt tolerance. Plant Physiol 131:676–683

Chen SR, Dickman MB (2004) Bcl-2 family members localize to tobacco chloroplasts and inhibit programmed cell death induced by chloroplast-targeted herbicides. J Exp Bot 55:2617–2623

Chen Z, Newman I, Zhou M, Mendham N, Zhang G, Shabala S (2005) Screening plants for salt tolerance by measuring K^+ flux: a case study for barley. Plant Cell Environ 28:1230–1246

Chen ZH, Zhou MX, Newman IA, Mendham NJ, Zhang GP, Shabala S (2007) Potassium and sodium relations in salinised barley tissues as a basis of differential salt tolerance. Funct Plant Biol 34:150–162

Chichkova NV, Kim SH, Titova ES, Kalkum M, Morozov VS, Rubtsov YP, Kalinina NO, Taliansky ME, Vartapetian AB (2004) A plant caspase-like protease activated during the hypersensitive response. Plant Cell 16:157–171

Clough SJ, Fengler KA, Yu I-C, Lippok B, Smith RK, Bent AF (2000) The *Arabidopsis dnd1* ''defense, no death'' gene encodes a mutated cyclic nucleotide-gated ion channel. Proc Natl Acad Sci USA 97:9323–9328

Cuin TA, Shabala S (2005) Exogenously supplied compatible solutes rapidly ameliorate NaCl-induced potassium efflux from barley roots. Plant Cell Physiol 46:1924–1933

Cuin TA, Miller AJ, Laurie SA, Leigh RA (2003) Potassium activities in cell compartments of salt-grown barley leaves. J Exp Bot 54:657–661

Demidchik V, Shabala SN, Coutts KB, Tester MA, Davies JM (2003) Free oxygen radicals regulate plasma membrane Ca^{2+} and K^+-permeable channels in plant root cells. J Cell Sci 116:81–88

Dickman MB, Park YK, Oltersdorf T, Li W, Clemente T, French R (2001) Abrogation of disease development in plants expressing animal antiapoptotic genes. Proc Natl Acad Sci USA 98:6957–6962

Gulbins E, Jekle A, Ferlinz K, Grassme H, Lang F (2000) Physiology of apoptosis. Am J Physiol Renal Physiol 279:F605–F615

Hatsugai N, Kuroyanagi M, Yamada K, Meshi T, Tsuda S, Kondo M, Nishimura M, Hara-Nishimura I (2004) A plant vacuolar protease, VPE, mediates virus-induced hypersensitive cell death. Science 305:855–858

Hughes FM, Cidlowski JA (1999) Potassium is a critical regulator of apoptotic enzymes in vitro and in vivo. Adv Enzyme Regul 39:157–171

Huh G-H, Damsz B, Matsumoto TK, Reddy MP, Rus AM, Ibeas JI, Narasimhan ML, Bressan RA, Hasegawa PM (2002) Salt causes ion disequilibrium-induced programmed cell death in yeast and plants. Plant J 29:649–659

Katsuhara M, Kawasaki T (1996) Salt stress induced nuclear and DNA degradation in meristematic cells of barley roots. Plant Cell Physiol 37:169–173

Khurana SMP, Pandey SK, Sarkar D, Chanemougasoundharam A (2005) Apoptosis in plant disease response: a close encounter of the pathogen kind. Curr Sci 88:740–752

Lam E, Kato N, Lawton M (2001) Programmed cell death, mitochondria and the plant hypersensitive response. Nature 411:848–853

Li W, Dickman MB (2004) Abiotic stress induces apoptotic-like features in tobacco that is inhibited by expression of human Bcl-2. Biotechnol Lett 26:87–95

Lincoln JE, Richael C, Overduin B, Smith K, Bostock R, Gilchrist DG (2002) Expression of the antiapoptotic baculovirus p35 gene in tomato blocks programmed cell death and provides broad-spectrum resistance to disease. Proc Natl Acad Sci USA 99:15217–15221

Maathuis FJM, Amtmann A (1999) K^+ nutrition and Na^+ toxicity: the basis of cellular K^+/Na^+ ratios. Ann Bot 84:123–133

Marschner H (1995) Mineral nutrition of higher plants, 2nd edn. Academic, London

McKersie BD, Hucl P, Beversdorf WD (1982) Solute leakage from susceptible and tolerant cultivars of *Phaseolus vulgaris* following ozone exposure. Can J Bot 60:73–78

Mitsuhara I, Malik KA, Miura M, Ohashi Y (1999) Animal cell-death suppressors Bcl-x(L) and CED-9 inhibit cell death in tobacco plants. Curr Biol 14:775–778

Newman IA (2001) Ion transport in roots: measurement of fluxes using ion-selective microelectrodes to characterize transporter function. Plant Cell Environ 24:1–14

Panayiotidis MI, Bortner CD, Cidlowski JA (2006) On the mechanism of ionic regulation of apoptosis: would the Na^+/K^+-ATPase please stand up? Acta Physiol 187:205–215

Pang JY, Zhou MX, Mendham N, Shabala S (2004) Growth and physiological responses of six barley genotypes to waterlogging and subsequent recovery. Aust J Agric Res 55:895–906

Pennell RI, Lamb C (1997) Programmed cell death in plants. Plant Cell 9:1157–1168

Qiao J, Mitsuhara I, Yazaki Y, Sakano K, Gotoh Y, Miura M, Ohashi Y (2002) Enhanced resistance to salt, cold and wound stresses by overproduction of animal cell death suppressors Bcl-xL and CED-9 in tobacco cells—their possible contribution through improved function of organella. Plant Cell Physiol 43:992–1005

Rojo E, Martin R, Carter C, Zouhar J, Pan SQ, Plotnikova J, Jin HL, Paneque M, Sanchez-Serrano JJ, Baker B, Ausubel FM, Raikhel NV (2004) VPE gamma exhibits a caspase-like activity that contributes to defense against pathogens. Curr Biol 14:1897–1906

Scholthof HB, Scholthof KBG, Jackson AO (1996) Plant virus gene vectors for transient expression of foreign proteins in plants. Annu Rev Phytopathol 34:299–323

Shabala L, Cuin TA, Newman IA, Shabala S (2005) Salinity-induced ion flux patterns from the excised roots of *Arabidopsis sos* mutants. Planta 222:1041–1050

Shabala S (2000) Ionic and osmotic components of salt stress specifically modulate net ion fluxes from bean leaf mesophyll. Plant Cell Environ 23:825–837

Shabala S, Babourina OK, Newman IA (2000) Ion-specific mechanisms of osmoregulation in bean mesophyll cells. J Exp Bot 51:1243–1253

Shabala S, Demidchik V, Shabala L, Cuin TA, Smith SJ, Miller AJ, Davies JM, Newman IA (2006) Extracellular Ca^{2+} ameliorates NaCl-induced K^+ loss from *Arabidopsis* root and leaf cells by controlling plasma membrane K^{+-}permeable channels. Plant Physiol 141:1653–1665

Shabala S, Newman IA, Morris J (1997) Oscillations in H^+ and Ca^{2+} ion fluxes around the elongation region of corn roots and effects of external pH. Plant Physiol 113:111–118

Shabala S, Shabala L, Van Volkenburgh E (2003) Effect of calcium on root development and root ion fluxes in salinised barley seedlings. Funct Plant Biol 30:507–514

Smethurst CF, Shabala S (2003) Screening methods for waterlogging tolerance in lucerne: comparative analysis of waterlogging effects on chlorophyll fluorescence, photosynthesis, biomass and chlorophyll content. Funct Plant Biol 30:335–343

Watanabe N, Lam E (2004) Recent advance in the study of caspase-like proteases and Bax inhibitor-1 in plants: their possible roles as regulator of programmed cell death. Mol Plant Pathol 5:65–70

Xu P, Rogers SJ, Roossinck MJ (2004) Expression of antiapoptotic genes *bcl- xL* and *CED- 9* in tomato enhances tolerance to viral-induced necrosis and abiotic stress. Proc Natl Acad Sci USA 101:15805–15810

Zhu JK (2002) Salt and drought stress signal transduction in plants. Annu Rev Plant Biol 53:247–273

Zimmermann S, Ehrhardt T, Plesch G, Mueller-Roeber B (1999) Ion channels in plant signaling. Cell Mol Life Sci 55:183–203